

**Observation of antisymmetric shock waves in soap-film flows**Yu Zhao  and Haitao Xu <sup>\*</sup>*Center for Combustion Energy and School of Aerospace Engineering,  
Tsinghua University, Beijing 100084, China*(Received 10 October 2021; revised 3 January 2022; accepted 19 July 2022;  
published 8 August 2022)

Objects inserted in a fast-flowing soap film are observed to cause strong disturbances on the film, resembling shock waves. Currently a prevailing opinion is that these shock waves correspond to sudden increases in film thickness caused by elastic symmetric waves, or the propagation of film thickness changes driven by surface tension variations with the film surface area. Here, we show by laser interferometry that these “shock waves” in fact originate from the antisymmetric waves studied by Taylor, which correspond to the bending of the liquid film with no thickness change. This phenomenon thus forms an example of symmetry breaking. These shock waves maintain an antisymmetric structure, but the structure size varies with the size of the intruding object. Our results indicate that these structures could be objects for studying solitary waves, rather than the traditional shocks corresponding to density jumps in compressible flows.

DOI: [10.1103/PhysRevFluids.7.L082001](https://doi.org/10.1103/PhysRevFluids.7.L082001)

The flow of liquid films is an intriguing problem that involves the interplay between fluid mechanics, surfactant transport, and interfacial phenomena. It is also ubiquitous, ranging from semiconductor manufacturing [1] to biophysics [2]. Among them, freely flowing soap films are probably the most common and are intensively studied. The dynamics of a soap film is tightly coupled to its shape and thickness, which cause fascinating optical effects, including the remarkable branched flow of light observed recently [3]. In soap films, disturbances in either the shape or the thickness of the liquid film propagate in the form of waves. There exist three kinds of waves (see Fig. 1): the antisymmetric Taylor waves that propagate at a speed of  $v_{AS} = \sqrt{2\sigma/\rho h}$ , the symmetric Taylor waves at speed  $v_S = k\sqrt{\sigma h/2\rho}$ , and the elastic symmetric waves at  $v_E = \sqrt{2E/\rho h}$ , in which  $\sigma$ ,  $\rho$ , and  $h$  are the surface tension, density, and thickness of the (undisturbed) soap film,  $k$  is the wave number, and  $E$  is the soap-film elasticity. While the first two wave modes also exist in films of pure water as shown in the classical work by Taylor [4], the third mode can only exist in soap films with surface tension coefficients varying with surface area, i.e., with nonzero elasticity  $E = A(d\sigma/dA)$ , in which  $A$  is the surface area of the film [5–7]. For freely flowing soap films, their thicknesses are typically in the order of micrometers, much shorter than the disturbance wavelengths, which means that the symmetric Taylor mode can be neglected compared to the antisymmetric mode since  $v_S/v_{AS} \sim kh \ll 1$ . Thus observing and distinguishing the antisymmetric Taylor waves and the elastic symmetric waves in flowing soap films has long been a research focus [8–13].

For gravity-driven, fast flowing soap films, it has been demonstrated that inserting a round rod into the film could generate a shock wave with an apparent Mach angle  $\alpha = \arcsin(1/\text{Ma}) = \arcsin(v/u)$ , where  $\text{Ma} = u/v$  is the Mach number, and  $v$  and  $u$  are the speeds of the propagating wave and the incoming flow, respectively. In the literature, this kind of shock wave is commonly

<sup>\*</sup>hxu@tsinghua.edu.cn

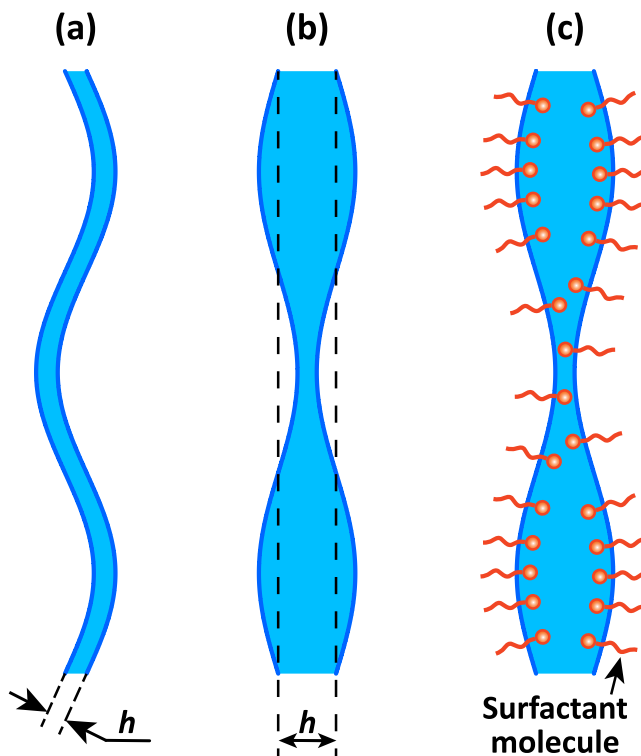


FIG. 1. Schematics of waves in soap films. (a) Antisymmetric Taylor waves, (b) symmetric Taylor waves, and (c) elastic symmetric waves. The elastic symmetric waves in (c) can only exist in soap films with surface tension varying with surface area, i.e., with nonzero  $d\sigma/dA$ .

reported as coming from the elastic symmetric waves and having a sudden increase in film thickness at the shock [11,13]. In this Letter, we show that this kind of shock in fact comes from the antisymmetric waves and there is no sharp change in film thickness across the shock. From this perspective, these are not traditional shock waves and are actually much closer to solitary waves formed by the superposition of antisymmetric waves.

The experiments were performed in a two-dimensional (2D) soap-film tunnel formed by two nylon wires as sketched in Fig. 2(a), a setup widely used for studying 2D flows [11–21]. In our experiment, a peristaltic pump was used to circulate the soap solution and set up the volume flow rate  $Q$ , and the separation width between two nylon wires was  $W = 2$  cm. The soap solution consisted of 2% Dawn detergent, 10% glycerol, and 88% de-ionized water, all in mass, which is the “standard” recipe for soap-film flows [11–14,16,17,20,21]. At this concentration, the active surfactant (sodium dodecyl sulfate, SDS) is in the high-concentration regime [12,13,16,22–26], i.e., its bulk concentration is higher than the critical micelle concentration (CMC), which means that the surface tension  $\sigma$  of the soap film, when its surfactant concentrations on the interface and in the bulk are at equilibrium, is saturated to a constant and no longer varies with the bulk concentration [23,27–30]. When a round rod is inserted into this flowing soap film, if the film speed is large enough, a shock wave can be formed around the rod, with reflections at the vertical boundaries. In this Letter, we focus on the primary shock wave near the rod.

To have more information on the film thickness, especially when the shock was formed, we used laser interferometry to examine the change of film thickness around the rod [Fig. 2(b)]. The incident light was a collimated beam from a cw solid-state laser with a wavelength of  $\lambda = 671$  nm and a power of 5 W. The laser beam and a high-speed camera (Phantom VEO710, VisionResearch,

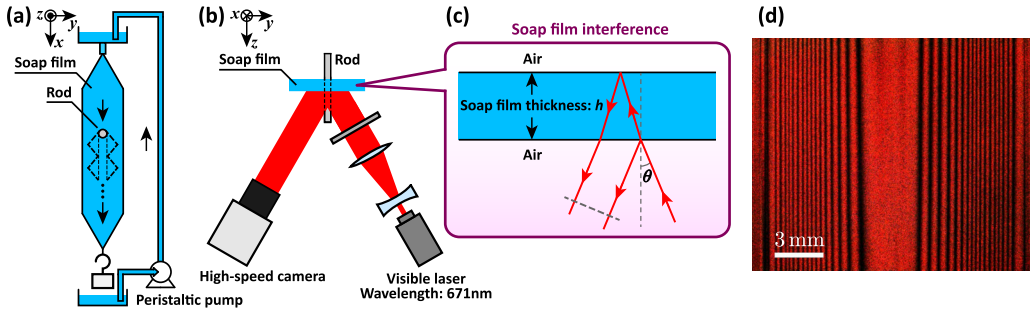


FIG. 2. Schematics of the soap-film flow setup and the laser interferometry to reveal the change of film thickness. (a) The soap-film flow. The gravity-driven soap-film flow is confined by two nylon wires with diameters of 0.32 mm held by hooks and weights. The peristaltic pump circulates the soap solution and sets up its volume flow rate. (b) Optical setup of the laser interferometry. (c) The corresponding optical path. (d) An example interference image of an undisturbed soap film.

Inc.) were placed on the same side of the soap film at the same angle  $\theta = 9.5^\circ$  to the film. The images captured by the camera were formed by the interference between the reflected lasers from the front and back surfaces of the film [Fig. 2(c)]. Each interference fringe thus corresponds to an isopach of the soap film at an thickness of  $h = m\lambda/2\sqrt{n^2 - \sin^2\theta}$ , where  $m = 0, 1, 2, \dots$  is the order of the black interference fringe and  $n$  is the refractive index of the soap solution. Figure 2(d) is an example image of the interference image formed by an undisturbed flowing soap film, of which the volume flow rate of the soap solution was  $Q = 35$  ml/min and the film thickness in the center was  $h = 8.7$   $\mu\text{m}$ , measured by an infrared absorption method similar to that reported before for soap-film flows [31].

For the shock wave formed by inserting a rod into the film, if the film thickness suddenly changes at the shock, the interference fringes should become discontinuous at the shock. However, as we show now, this is not the case for the entire range of Mach numbers that we tested. Figure 3 shows the interference fringes after inserting a rod with diameter  $D = 650$   $\mu\text{m}$  into the film. From Figs. 3(a) to 3(f), the volume flow rate was increased from  $Q = 20$  ml/min to  $Q = 45$  ml/min, which resulted in an increase in the Mach number and hence a decrease in the Mach angle. For all these cases it is clearly seen that the interference fringes were continuous across the shock wave, as shown in the closeup view on the right-hand side of each panel in Fig. 3. (Note that as mentioned before, there were reflections of the shock wave at the boundaries of the soap film formed by the nylon wires, which we do not discuss here.) The bending of the fringes in the shock region was due to the deformation of the film, very much as a “curtain pleat,” as illustrated in Fig. 4.

The images above thus give strong support that these shock waves originated from the superposition of the antisymmetric Taylor waves rather than the elastic symmetric waves.

We note that if the shock waves were caused by elastic symmetric waves, one could estimate the film elasticity  $E$  using the flow speed  $u$ , the Mach angle  $\alpha$ , and the film thickness  $h$  by  $E = \frac{1}{2}\rho h(u \sin \alpha)^2$ . Using data corresponding to the flowing soap films shown in Fig. 3 above, we estimated that  $E \approx 20$  mN/m. The film elasticity  $E = (d\sigma/d \ln A)$ , on the other hand, depends on how the surface tension responds to the relative change of the surface area, which involves the complicated process of surfactant migration between the interface and the interstitial fluid.

If the area variation is relatively slow so that the surfactant concentration on the film interface always remains at equilibrium with the bulk surfactant concentration of the interstitial fluid, which is the so-called Gibbs regime [7], the film elasticity can be estimated from the dependence of surface tension on the surfactant concentration in the bulk fluid. For soap films created from soap solutions with a surfactant concentration above the CMC, the surface tension is nearly independent of the surfactant concentration [7,30], which implies that the Gibbs elasticity of a soap film under this

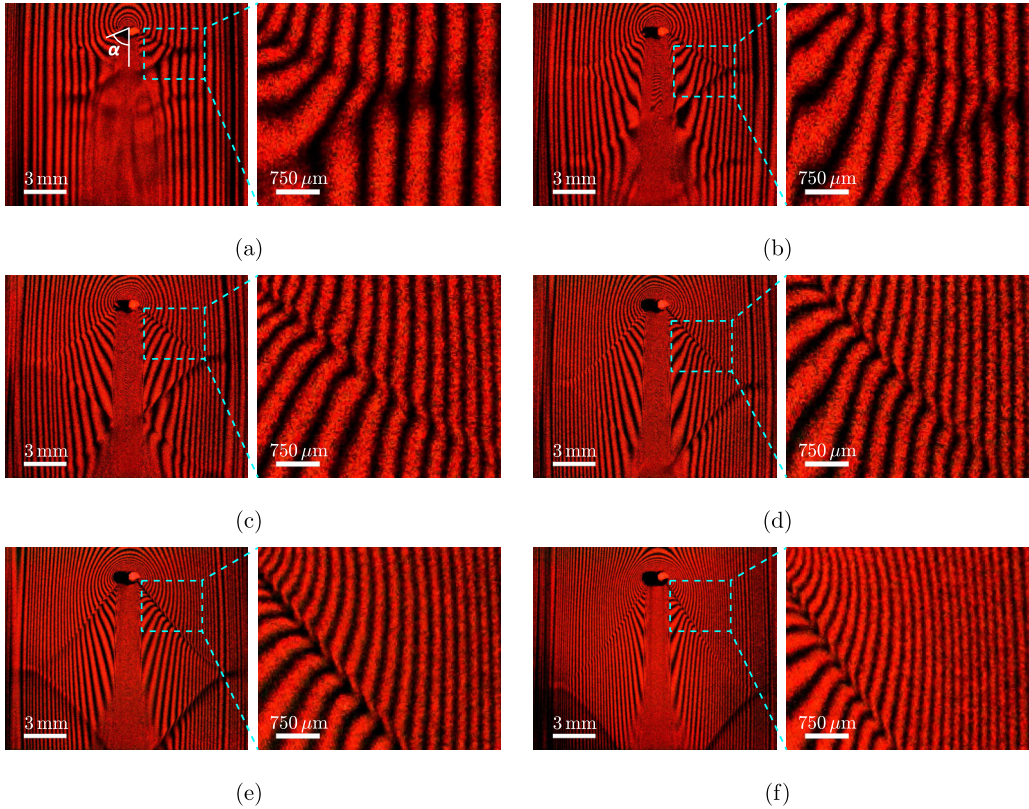


FIG. 3. The interference fringes over flowing soap films with shock waves formed by inserting a rod with diameter  $D = 650 \mu\text{m}$ . The volume flow rate of the soap solution  $Q$  for the flow shown in each panel is (a) 20 ml/min, (b) 25 ml/min, (c) 30 ml/min, (d) 35 ml/min, (e) 40 ml/min, and (f) 45 ml/min, with the Mach angle  $\alpha$  respectively at  $69^\circ$ ,  $55^\circ$ ,  $47^\circ$ ,  $41^\circ$ ,  $37^\circ$ , and  $34^\circ$ . In each panel, a closeup view of the continuous interference fringes across the shock is shown on the right.

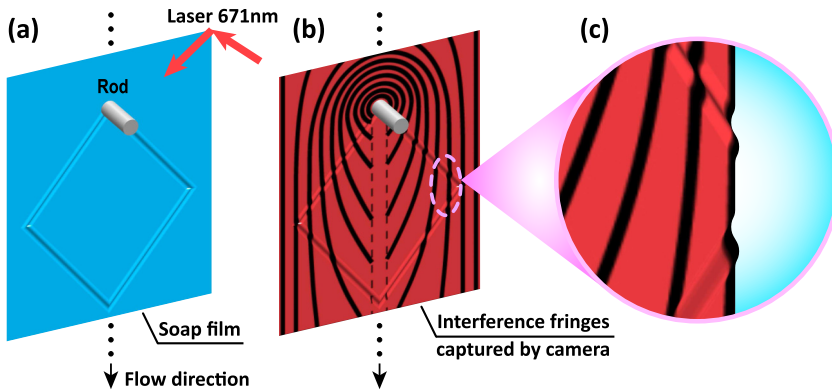


FIG. 4. A sketch to illustrate the interference fringes over the shock. (a) The formation of shock waves by the insertion of a round rod in a supersonic soap-film flow and the reflection at the boundary. (b) The corresponding interference fringes. (c) A closeup and cut-through view of the soap film that shows the deformation of the film and the interference fringes.

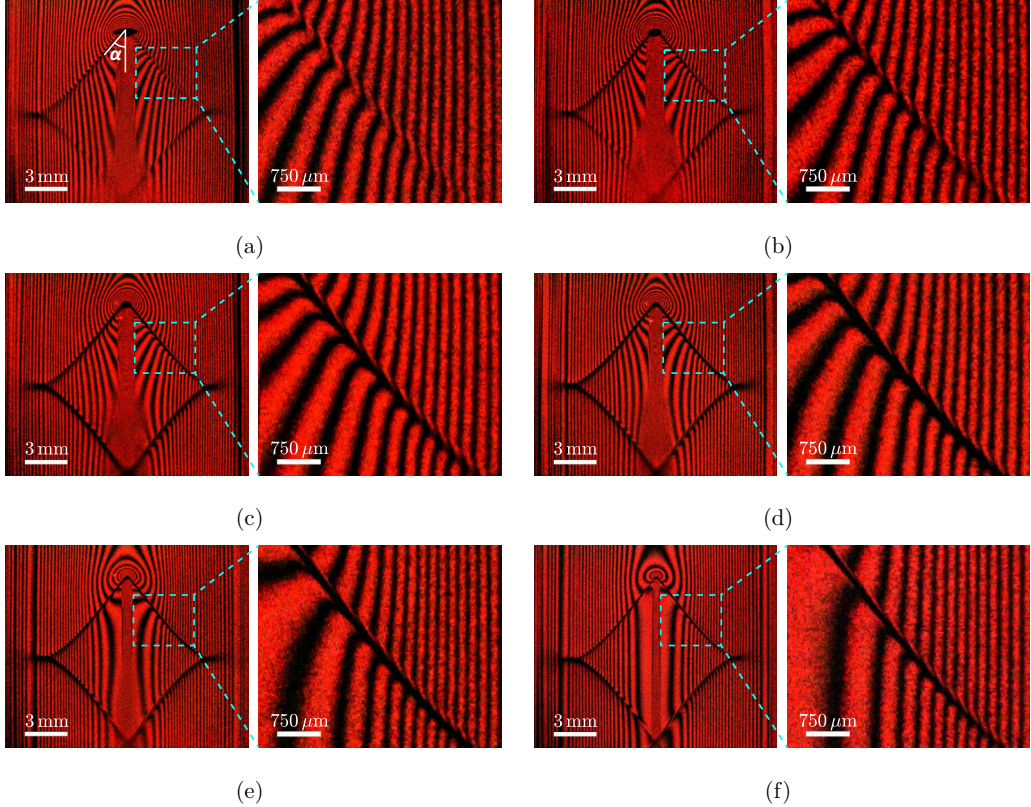


FIG. 5. The interference fringes of 35 ml/min flowing soap films with magnification (as shown by the scale bars), in which the inserted diameter  $D$  of the conical needle is (a) 450  $\mu\text{m}$ , (b) 420  $\mu\text{m}$ , (c) 350  $\mu\text{m}$ , (d) 250  $\mu\text{m}$ , (e) 150  $\mu\text{m}$ , and (f) 50  $\mu\text{m}$ .

condition is  $E_G \approx 0$ . Using the surface tension data measured from deforming soap bubbles [30], it can be estimated that  $E_G \lesssim 4$  mN/m, which is too small compared to that required by the observed Mach angle.

If the area variation of the soap film is very fast so that the same number of surfactant molecules remain on the interface during the surface deformation, this is called the Marangoni regime [7]. The film elasticity in this case then depends on the rate of surface stretching. For the distortion of the film caused by the flow past an object, by dimensional analysis, the rate of film stretching ( $d \ln A / dt$ ) should depend on  $u/D$ , where  $u$  is the speed of the film flow and  $D$  is the characteristic size of the object. Therefore, by varying the diameter  $D$  of the rod inserted in the film while keeping the flow rate  $Q$  the same, we could evaluate the effect of film elasticity on the response of the film to the disturbance.

Figures 5(a)–5(f) show the interference fringes when the diameter of the intrusion was decreased from  $D = 450$   $\mu\text{m}$  to 50  $\mu\text{m}$ , while the volume flow rate of the soap film was kept fixed at  $Q = 35$  ml/min. The diameter  $D$  was varied by moving a conical needle inserted into the soap film perpendicular to the film along a precision translation stage. Note that as the cone angle of the needle was  $15^\circ$  and the thickness of the soap film was  $\sim 10$   $\mu\text{m}$ , the change of diameter  $D$  within the soap film due to the conical shape of the needle was only approximately 2  $\mu\text{m}$ , which was insignificant for  $50$   $\mu\text{m} \leq D \leq 450$   $\mu\text{m}$ . For large  $D$ , such as Fig. 5(a) with  $D = 450$   $\mu\text{m}$ , the interference fringes look very similar to those disturbed by the rod shown in Fig. 3 and can be seen to be clearly continuous across the shock or the “pleat” as sketched in Fig. 4. When  $D$  was

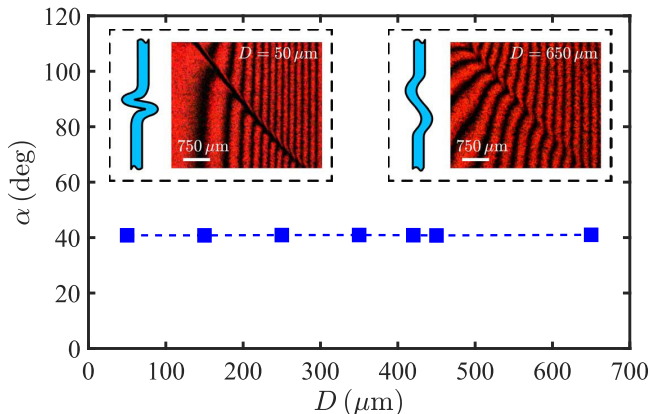


FIG. 6. The Mach angle  $\alpha$  (i.e., the half angle of Mach cone) under 35 ml/min flow rate with different inserted diameters  $D$  of the conical needle. The Mach angle  $\alpha$  is independent of the inserted needle diameter  $D$  and remains constant under a fixed flow rate  $Q$ .

decreased, the amplitude-to-width ratio of the pleat increased, which made the fringes in the shock region less distinguishable. At  $D = 50 \mu\text{m}$ , the amplitude-to-width ratio was so large that the fringes bent abruptly across the shock and seemed to have joined together at the shock wave (we remark that it can be seen that there was still a clear one-to-one correspondence between the fringes on the two sides of the shock), which could be mistakenly regarded as indicating a sudden increase in film thickness. This might be the main reason why existing views consider this kind of shock wave as originating from elastic symmetric waves. Physically, this just means that the amplitude of the antisymmetric shock wave is much larger than its wavelength, which makes the soap film bend to almost self-merging, but this is fundamentally not a film thickness increase due to elastic symmetric waves.

In Fig. 6, we plot the Mach angle  $\alpha = \arcsin(1/\text{Ma}) = \arcsin(v/u)$  measured from images as those shown in Fig. 5, together with  $\alpha$  measured from Fig. 3(d), which were obtained at the same flow rate as those in Fig. 5, but with  $D = 650 \mu\text{m}$ . Under a fixed flow rate  $Q$ , or flow speed  $u$ , the Mach angle  $\alpha$  is independent of the inserted diameter  $D$ , which means that the rate of film stretching has no effect on the shock-wave generation mechanism. Moreover, using the flow rate  $Q = 35 \text{ ml/min}$ , film width  $W = 2 \text{ cm}$ , film thickness  $h = 8.7 \mu\text{m}$ , density of the soap solution  $\rho = 1.026 \text{ g/cm}^3$ , and the value of the surface tension  $\sigma = 22 \text{ mN/m}$  for soap film at this detergent concentration [30], the Mach angle can be calculated as  $\alpha = \arcsin(v_{AS}/u) = \arcsin(\sqrt{2\sigma h/\rho W}/Q) = 41.5^\circ$ , which agrees well with the measured value as shown in Fig. 6. Thus Fig. 6 and the calculation above provide quantitative evidence that the shocks observed resulted from the propagation of the antisymmetric Taylor waves, not the elastic symmetric waves.

In summary, we showed that typical shock waves behind intrusions in a flowing soap film actually originate from the superposition of the antisymmetric Taylor waves, rather than the elastic symmetric waves as commonly thought. As the flow is symmetric about the middle plane of the soap film, it is natural to think that the disturbed waves are also symmetric, which is indeed the prevailing opinion. However, our results indicate that the flow chooses a symmetry-breaking state under the perturbation by an intrusion. This symmetry-breaking behavior is worthy of further investigation.

We note that the ‘‘shock waves’’ discussed are not the traditional shocks in aerodynamics as there are no appreciable changes of flow velocity or film thickness (which acts as density for film flows) across the shock as regarded before [11, 13]. The dominating feature is the sinusoidal antisymmetric waves with very large amplitudes, which highly resemble solitary waves rather than shocks. Our results thus indicate an object for the study of solitary waves in the future.

We are thankful to Dr. Z. Zhou for his contribution in the setup of the soap-film flow facility, and to Prof. A. Pumir for suggestions and discussions. This work is supported partially by the Natural Science Foundation of China (NSFC) through Grant No. 11988102 and by Tsinghua University.

- [1] M. Quirk and J. Serda, *Semiconductor Manufacturing Technology* (Prentice Hall, Hoboken, NJ, 2001).
- [2] A. Oron, S. H. Davis, and S. G. Bankoff, Long-scale evolution of thin liquid films, *Rev. Mod. Phys.* **69**, 931 (1997).
- [3] A. Patsyk, U. Sivan, M. Segev, and M. A. Bandres, Observation of branched flow of light, *Nature (London)* **583**, 60 (2020).
- [4] G. I. Taylor, The dynamics of thin sheets of fluid II. Waves on fluid sheets, *Proc. R. Soc. London, Ser. A* **253**, 296 (1959).
- [5] J. Lucassen, M. Van den Tempel, A. Vrij, and F. Hesselink, Waves in thin liquid films I. The different modes of vibrations, *Proc. K. Ned. Akad. Wet. Ser. B: Phys. Sci.* **73**, 109 (1970).
- [6] A. Vrij, F. Hesselink, J. Lucassen, and M. Van den Tempel, Waves in thin liquid films II. Symmetrical modes in very thin films and film ruptures, *Proc. K. Ned. Akad. Wet. Ser. B: Phys. Sci.* **73**, 124 (1970).
- [7] Y. Couder, J. M. Chomaz, and M. Rabaud, On the hydrodynamics of soap films, *Physica D* **37**, 384 (1989).
- [8] C. Y. Wen, Y. M. Chen, and S. K. Chang-Jian, A soap film shock tube to study two-dimensional compressible flows, *Exp. Fluids* **31**, 19 (2001).
- [9] C. Y. Wen and J. Y. Lai, Analogy between soap film and gas dynamics. I. Equations and shock jump conditions, *Exp. Fluids* **34**, 107 (2003).
- [10] C. Y. Wen, S. K. Chang-Jian, and M. C. Chuang, Analogy between soap film and gas dynamics. II. Experiments on one-dimensional motion of shock waves in soap films, *Exp. Fluids* **34**, 173 (2003).
- [11] T. Tran, P. Chakraborty, G. Gioia, S. Steers, and W. I. Goldburg, Marangoni Shocks in Unobstructed Soap-Film Flows, *Phys. Rev. Lett.* **103**, 104501 (2009).
- [12] I. Kim and X. L. Wu, Tunneling of micron-sized droplets through soap films, *Phys. Rev. E* **82**, 026313 (2010).
- [13] I. Kim and S. Mandre, Marangoni elasticity of flowing soap films, *Phys. Rev. Fluids* **2**, 082001(R) (2017).
- [14] M. Rivera, P. Vorobieff, and R. E. Ecke, Turbulence in Flowing Soap Films: Velocity, Vorticity, and Thickness Fields, *Phys. Rev. Lett.* **81**, 1417 (1998).
- [15] J. Zhang, S. Childress, A. Libchaber, and M. Shelley, Flexible filaments in a flowing soap film as a model for one-dimensional flags in a two-dimensional wind, *Nature (London)* **408**, 835 (2000).
- [16] M. A. Rutgers, X. L. Wu, and W. B. Daniel, Conducting fluid dynamics experiments with vertically falling soap films, *Rev. Sci. Instrum.* **72**, 3025 (2001).
- [17] H. Kellay and W. I. Goldburg, Two-dimensional turbulence: a review of some recent experiments, *Rep. Prog. Phys.* **65**, 845 (2002).
- [18] L. B. Jia and X. Z. Yin, Passive Oscillations of Two Tandem Flexible Filaments in a Flowing Soap Film, *Phys. Rev. Lett.* **100**, 228104 (2008).
- [19] T. Schnipper, A. Andersen, and T. Bohr, Vortex wakes of a flapping foil, *J. Fluid Mech.* **633**, 411 (2009).
- [20] G. Boffetta and R. E. Ecke, Two-dimensional turbulence, *Annu. Rev. Fluid Mech.* **44**, 427 (2012).
- [21] Z. Y. Zhou, L. Fang, N. T. Ouellette, and H. T. Xu, Vorticity gradient stretching in the direct enstrophy transfer process of two-dimensional turbulence, *Phys. Rev. Fluids* **5**, 054602 (2020).
- [22] A. Prins, C. Arcuri, and M. Van den Tempel, Elasticity of thin liquid films, *J. Colloid Interface Sci.* **24**, 84 (1967).
- [23] H. Bianco and A. Marmur, Gibbs elasticity of a soap bubble, *J. Colloid Interface Sci.* **158**, 295 (1993).
- [24] E. Fuguet, C. Ràfols, M. Rosés, and E. Bosch, Critical micelle concentration of surfactants in aqueous buffered and unbuffered systems, *Anal. Chim. Acta* **548**, 95 (2005).
- [25] R. Sadeghi and S. Shahabi, A comparison study between sodium dodecyl sulfate and sodium dodecyl sulfonate with respect to the thermodynamic properties, micellization, and interaction with poly(ethylene glycol) in aqueous solutions, *J. Chem. Thermodyn.* **43**, 1361 (2011).

- [26] M. A. Motin, M. H. Mia, and A. N. Islam, Thermodynamic properties of sodium dodecyl sulfate aqueous solutions with methanol, ethanol, *n*-propanol and *iso*-propanol at different temperatures, *J. Saudi Chem. Soc.* **19**, 172 (2015).
- [27] F. Evans and W. Wennerström, *The Colloidal Domain* (Wiley, New York, 1999).
- [28] D. Langevin and F. Monroy, Marangoni stresses and surface compression rheology of surfactant solutions. achievements and problems, *Adv. Colloid Interface Sci.* **206**, 141 (2014).
- [29] D. Langevin, Rheology of adsorbed surfactant monolayers at fluid surfaces, *Annu. Rev. Fluid Mech.* **46**, 47 (2014).
- [30] D. M. Wan, H. S. Xiang, and H. T. Xu, A laminar-jet-discharging method for measuring the interfacial tension of deformable surfaces, *Meas. Sci. Technol.* **31**, 035302 (2020).
- [31] X.-L. Wu, R. Levine, M. Rutgers, H. Kellay, and W. I. Goldburg, Infrared technique for measuring thickness of a flowing soap film, *Rev. Sci. Instrum.* **72**, 2467 (2001).